



RNA
A PUBLICATION OF THE RNA SOCIETY

Crystal structure of an RNA duplex containing phenyl-ribonucleotides, hydrophobic isosteres of the natural pyrimidines.

G Minasov, J Matulic-Adamic, C J Wilds, et al.

RNA 2000 6: 1516-1528

References

Article cited in:

<http://rnajournal.cshlp.org/content/6/11/1516.abstract.html#related-urls>

Email alerting service

Receive free email alerts when new articles cite this article - sign up in the box at the top right corner of the article or [click here](#)

To subscribe to *RNA* go to:
<http://rnajournal.cshlp.org/subscriptions/>

REPORT

Crystal structure of an RNA duplex containing phenyl-ribonucleotides, hydrophobic isosteres of the natural pyrimidines

GEORGE MINASOV,¹ JASENKA MATULIC-ADAMIC,² CHRISTOPHER J. WILDS,^{1,3}
PETER HAEBERLI,² NASSIM USMAN,² LEONID BEIGELMAN,² and MARTIN EGLI^{1,3}

¹Department of Molecular Pharmacology and Biological Chemistry and The Drug Discovery Program,
Northwestern University Medical School, Chicago, Illinois 60611, USA

²Ribozyme Pharmaceuticals Inc., 2950 Wilderness Place, Boulder, Colorado 80301, USA

ABSTRACT

Chemically modified nucleotide analogs have gained widespread popularity for probing structure–function relationships. Among the modifications that were incorporated into RNAs for assessing the role of individual functional groups, the phenyl nucleotide has displayed surprising effects both in the contexts of the hammerhead ribozyme and pre-mRNA splicing. To examine the conformational properties of this hydrophobic base analog, we determined the crystal structure of an RNA double helix with incorporated phenyl ribonucleotides at 1.97 Å resolution. In the structure, phenyl residues are engaged in self-pairing and their arrangements suggest energetically favorable stacking interactions with 3′-adjacent guanines. The presence of the phenyl rings in the center of the duplex results in only moderate changes of the helical geometry. This finding is in line with those of earlier experiments that showed the phenyl analog to be a remarkably good mimetic of natural base function. Because the stacking interactions displayed by phenyl residues appear to be similar to those for natural bases, reduced conformational restriction due to the lack of hydrogen bonds with phenyl as well as alterations in its solvent structure may be the main causes of the activity changes with phenyl-modified RNAs.

Keywords: dangling end; hydrophobic base pairing; nucleic acid analog; RNA; stacking; structure–function; X-ray crystallography

INTRODUCTION

Oligonucleotide analogs composed of chemically modified building blocks are currently being evaluated as antisense and antigene reagents for in vitro and potential in vivo therapeutic applications (Crooke, 1998; Nielsen, 1999). In addition, antisense oligonucleotide analogs constitute ideal tools for high-throughput gene functionalization and validation of drug targets (Bennett & Cowser, 1999; Taylor et al., 1999; Myers & Dean, 2000). Alternative oligonucleotide pairing systems have also been generated as part of ongoing investigations concerning the etiology of natural DNA and RNA (Eschenmoser, 1999).

Besides numerous other applications, chemically modified oligonucleotides were used in the analysis of DNA bending (Strauss et al., 1996), the gold nanoparticle-based colorimetric detection of polynucleotides (Elghanian et al., 1997) and as artificial ribonucleases in the sequence-specific cleavage of RNA (Hall et al., 1996). Nucleoside or nucleotide analogs served as probes of enzyme specificity (Marquez et al., 1998; Morales & Kool, 1998; Ogawa et al., 2000) and as transition-state analog inhibitors of a base-excision DNA repair protein (Deng et al., 1997) and DNA restriction enzymes (Blättler et al., 1998). Substitution of a particular nucleotide in the catalytic core of the hammerhead ribozyme by residues carrying base analogs were shown to substantially enhance the rate of the chemical step of the phosphoryl transfer reaction in some cases (Burgin et al., 1996). For example, a U → pyridin-4-one substitution at position 7 led to a 12-fold rate increase. The role of individual functional groups on the cleavage-site pyrimidine C17 in stabilizing the hammer-

Reprint requests to: Martin Egli, Department of Biological Sciences, Vanderbilt University, Nashville, Tennessee 37235, USA; e-mail: martin.egli@vanderbilt.edu or Leonid Beigelman, Ribozyme Pharmaceuticals Inc., 2950 Wilderness Place, Boulder, Colorado 80301, USA; e-mail: lnb@rpi.com.

³New address: Department of Biological Sciences, Vanderbilt University, Nashville, Tennessee 37235, USA.

Structure of an RNA duplex with phenyl ribonucleotides

head transition-state structure were assessed by replacing cytosine with chemically modified pyrimidine analogs (Baidya et al., 1997). These experiments revealed that both carbonyl and amino group of C17 are required for stabilizing the transition state of the hammerhead-catalyzed cleavage reaction. However, the two exocyclic functional groups make little or no contribution to either substrate or product binding.

Both studies demonstrate the potential advantages of using chemically modified nucleotide analogs in the analysis of structure-function relationships compared with simple mutagenesis involving only natural nucleotides. An interesting result of these studies was

the change in activity observed with hammerheads containing the phenyl ribonucleotide analog that completely lacks base functions (Fig. 1A, phenyl ribonucleoside is compound 5). In place of residue U7, the phenyl nucleotide produced a twofold increase in the cleavage rate (Burgin et al., 1996). Similarly, the cleavage rate with a hammerhead ribozyme containing a phenyl residue instead of C17 was much higher than one would have expected (Baidya et al., 1997). Moreover, experiments were carried out that examined the possibility of activating mutated hammerhead ribozymes featuring abasic sites by adding exogenous base moieties (Peracchi et al., 1998). Replacement of adenine at position

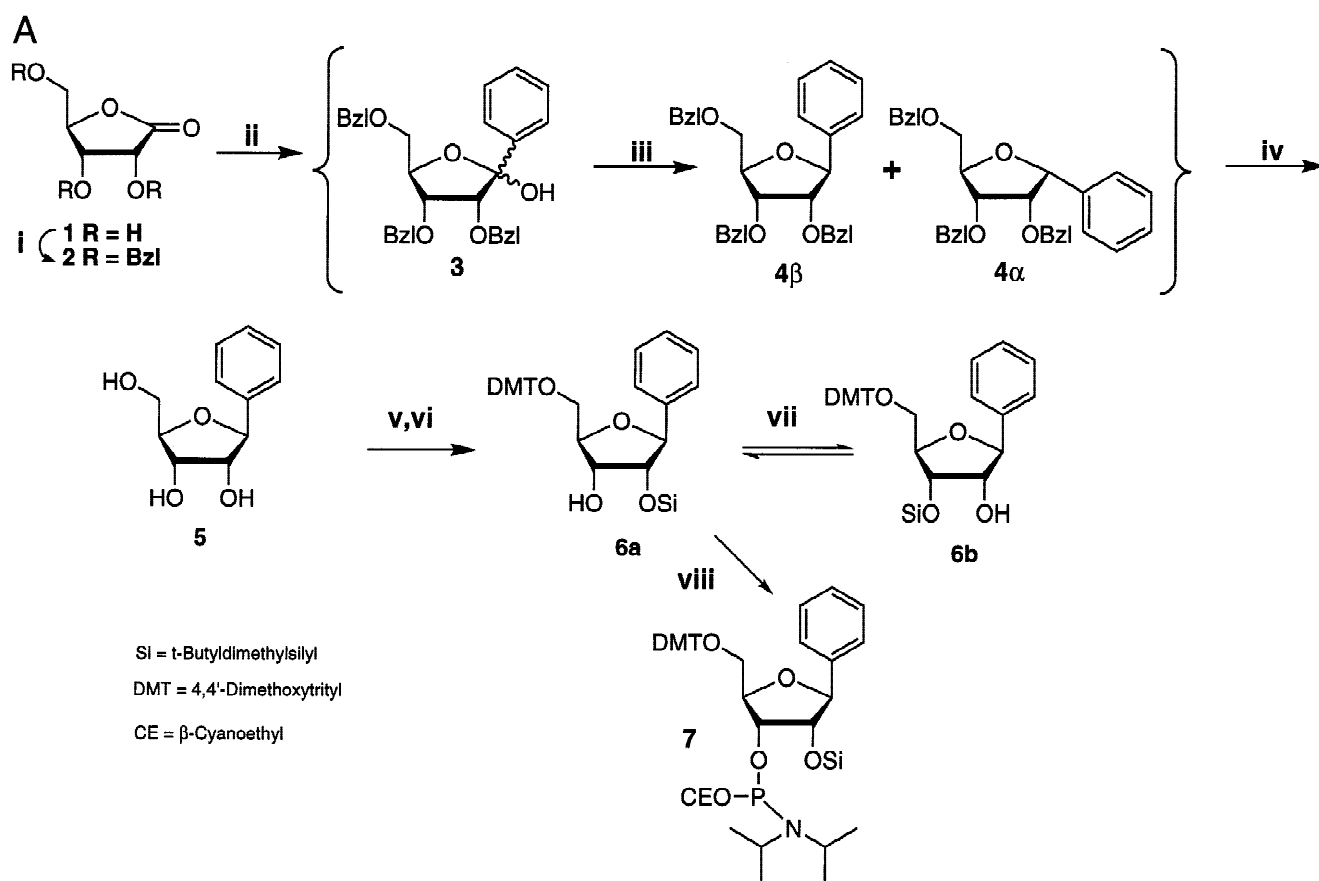
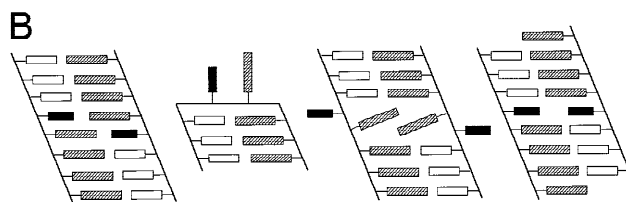


FIGURE 1. A: Preparation of 1-Deoxy-1-phenyl- β -D-ribofuranose derivative suitable for oligonucleotide synthesis; compound 5 corresponds to the phenyl ribonucleoside. Reagents: i: Triflic acid, benzyl 2,2,2-trichloroacetimidate; ii: Phenyllithium; -78°C ; iii: Triethylsilane, boron trifluoride etherate, -40°C ; iv: Boron tribromide, -78°C ; v: 4,4'-Dimethoxytrityl chloride, pyridine; vi: Silver nitrate, *t*-butyldimethylsilyl chloride, tetrahydrofuran/pyridine; vii: 5% Triethylamine in methanol; viii: 2-Cyanoethyl *N,N*-diisopropylchlorophosphoramidite, *N*-methylimidazole, *N,N*-diisopropylethylamine. **B:** Possible structures for single- and double-stranded arrangements of the RNA octamer CCCPGGGG. Cytosines are drawn as open boxes, guanines are dashed, and phenyls are black. From left to right: duplex with two P-G mismatches; hairpin with three C-G base pairs in the stem and a P-G loop; duplex with a central purine-purine base pair and looped-out Ps; duplex with strands slid along each other by one base-pair step, generating a central P-P pair and 3-terminal G overhangs. The arrangement on the far right is observed in the crystal structure.



9 with phenyl decreased the catalytic rate only 20-fold compared to the 2,000-fold deleterious effect resulting from removal of the adenine base. Another surprising observation was the almost wild-type activity of a nuclear pre-mRNA variant with an adenine \rightarrow phenyl mutation at the 3'-splice AG during the second step of the splicing reaction (Gaur et al., 2000).

The consequences of hydrophobic, non-hydrogen-bonding bases and base pairs for duplex stability and nucleic acid-protein interactions have been investigated in some detail with DNA but remain largely unexplored in the case of RNA. Thus, difluorotoluene (F), a nonpolar analog of thymine codes specifically for adenine replication (Moran et al., 1997) and the geometry of the F-A pair closely resembles that of T-A, although F causes destabilization of the DNA duplex (Guckian et al., 1998). Similarly, a pyrene nucleoside analog shows significant selectivity for a model abasic site over the natural bases (Matray & Kool, 1998) and polymerases efficiently incorporate the pyrene residue opposite a template site lacking a base (Matray & Kool, 1999). In DNA duplexes, nonpolar isosteres of adenine and thymine pair with a stability that is similar to that of the T-G mismatch base pair (Schweitzer & Kool, 1995). Moreover, at the ends of helices such hydrophobic pairs can be more stabilizing than a canonical A-T pair and, interestingly, hydrophobic analogs prefer to pair with a hydrophobic partner rather than a natural base. Attached at the 5'-terminus of a DNA duplex as single dangling nucleotides, nonpolar aromatic analogs were found to be equally or more stabilizing than the four natural bases (Guckian et al., 2000).

Here, we report a new chemical synthetic route for preparing the phenyl ribonucleotide. To shed light on the energetic and structural consequences of the incorporation of the phenyl nucleotide analog into an RNA duplex, we analyzed the thermodynamic stability of RNA octamers with single phenyl residues (P) and determined the crystal structure of r(CCCPGGGG). The structure gives the first detailed picture of the interactions of the hydrophobic phenyl nucleotide in the context of an RNA duplex and may aid in the rationalization of the accumulated activity data for RNAs bearing the phenyl modification.

RESULTS AND DISCUSSION

Synthesis of C-phenyl phosphoramidite 7

To determine the importance of stacking and hydrophobic interactions in the hammerhead system, we designed and synthesized the C-phenyl phosphoramidite (Fig. 1A, compound 7) (Matulic-Adamic et al., 1996). In this analog the pyrimidine base is substituted by a phenyl ring, rendering the nucleotide incapable of forming hydrogen-bonding contacts but still able to support stacking and hydrophobic interactions.

Our synthetic approach to the key intermediate 1-deoxy-1-phenyl- β -D-ribofuranose (Fig. 1A, compound 5) is based on previous work for highly stereoselective preparation of 1-deoxy-1-phenyl- β -D-glucopyranose from protected D-glucopyranolactone and phenyllithium (Czernecki & Ville, 1989). The choice of protecting groups for the starting ribonolactone is critical for this approach: they must be compatible with the highly reactive organometallic reagent and also withstand the strongly acidic conditions generated during reduction with $\text{Et}_3\text{SiH}/\text{BF}_3\text{Et}_2\text{O}$. We first developed a synthesis starting from 5-O-*tert*-butyldiphenylsilyl-2,3-O-isopropylidene-D-ribo-1,4-lactone (Matulic-Adamic et al., 1996) and later refined this approach using a shorter route through 2,3,5-tri-O-benzyl-D-ribo-1,4-lactone 2 (Fig. 1A), which we disclose in this communication.

The development of acid-catalyzed benzylation of aldonolactones (Jensen et al., 1997) allowed for the one-step preparation of 2,3,5-tri-O-benzyl-D-ribo-1,4-lactone (2) in 90% yield from commercially available D-ribo-1,4-lactone. Condensation of the protected lactone 2 with PheLi leads to a mixture of lactols 3 (Fig. 1A) that are reduced without isolation to an α : β mixture of protected C-nucleosides (4β and 4α , Fig. 1A). According to ^1H NMR, these two reactions provide predominantly the desired β anomer 4β in a ratio of α : β = 1:4 for the mixture. Monitoring the first step by thin-layer chromatography (TLC) requires several developments of the TLC plate in the provided system to achieve adequate resolution. We also recommend charring TLC plates at $>100^\circ\text{C}$ for visualizing carbohydrate precursors after development and dipping in a 1% solution of H_2SO_4 in ether. This technique proves useful for visualization of closely moving compounds with weak chromophores (i.e., benzylated sugars).

The mixture of C-phenyl nucleosides 4β and 4α can be separated and then 4β can be debenzylated to provide the target free nucleoside 5. In our hands the reverse sequence, debenylation of the mixture of 4β and 4α followed by separation of free nucleosides, proved to be more reproducible, as separation of 4β and 4α is quite tedious. Combining these three reactions in one procedure allows for only one chromatographic purification at the end and reproducibly provides gram quantities of C-phenyl riboside 5. Subsequent standard tritylation and silylation lead to a mixture of 5'-O-DMT 2'- and 3'-silyl isomers (6a and 6b; Fig. 1A) in an $\sim 1:1$ ratio with a small amount of bis-silylated product. Careful separation of these products by flash chromatography affords the faster running 3'-O-Si isomer (6b) followed by the 2'-O-Si isomer (6a). It is worth noting that the 3'-O-Si isomer in this case is faster moving than the 2'-O-Si isomer, unlike the majority of *tert*-butyldimethylsilylated 5'-O-DMT derivatives of ribonucleosides.

Because the ratio of silyl isomers during silylation of the 5'-O-DMT intermediate is close to 1:1, it is worth-

while to re-isomerise the isolated undesired 3'-*O*-Si isomer (6b) to the mixture of 2'- and 3'-*O*-Si compounds. The routinely used mixture of 5–10% pyridine in methanol overnight (Ogilvie, 1983) does not produce any isomerization; however, 5% Et₃N in methanol, in 1 h, results in a 1:1 mixture of 2':3'-isomers that are separated again to provide an additional amount of the target 2'-*O*-Si isomer. These isomerization conditions are general (data not shown) and we recommend this procedure for equilibration of 3'-*O*-Si-isomers of different analogs during large-scale (5–10 g) preparations or for occasions when unfavorable 3'-*O*-regioselectivity is observed. This simple approach allows for maximizing the yields of the desired 2'-*O*-Si intermediates. Standard phosphorylation then completes the synthesis of phosphoramidite 7 (Fig. 1A).

Overview of the structure

The phenyl-modified RNA octamer adopts a double-helical conformation in the crystal. The duplex is located on a twofold rotation axis and, therefore, a single strand constitutes the crystallographic asymmetric unit in the hexagonal lattice. Rather than forming P-G "pairs" (Fig. 1B, left), the phenyl moieties are arranged opposite each other in the center of the duplex (Fig. 1B, right). Thus, paired octamers have shifted along each other by 1 bp, resulting in the formation of six C-G base pairs, a central P-P pair, and overhanging guanines at the 3'-termini (Fig. 2A). The helix displays A-type geometry as expected for RNA and the presence of phenyl residues results only in minor deviations from the canonical A-form helical parameters. The two phenyl rings are in van der Waals contact with each other; the shortest distance between carbon atoms from opposite rings is 3.7 Å (C3...C3, Figs. 2B, 3). Therefore, the hydrophobic phenyl pair can be accommodated in the central section without locally reducing the diameter of the duplex (Fig. 2B). The distance between phosphorus atoms from opposite strands at PpG steps is 16.8 Å, and thus very similar to the average distance of 17.0 Å between phosphorus atoms of base pair steps in the rest of the duplex.

In the lattice, duplexes form infinite columns with dangling Gs from adjacent molecules stacked on one another. These stacking interactions and additional lateral contacts between duplexes are stabilized by Ca²⁺ ions that form inner and outer sphere contacts to terminal guanines and phosphate groups. Further stabilizing contacts between duplexes in the lattice are mediated by so-called ribose zippers (Cate et al., 1996), involving hydrogen bonds between 2'-hydroxyl groups from adjacent backbones. For analyzing the RNA duplex, nucleotides of single strands were numbered 1 to 8 and lower case letters mark residues from symmetry mates. The rhombohedral crystal form of the native RNA duplex [r(CCCCGGGG)]₂, determined to 1.45 Å resolu-

tion, served as the reference structure (Egli et al., 1996; Nucleic Acid Database code ARH074).

Helical parameters and backbone geometry

Consistent with the A-form geometry of the helix, all riboses adopt a C3'-*endo* conformation. The average amplitude of the pseudorotation phase angle *P* is 40° [calculated with the program CURVES (Lavery & Sklenar, 1989, 1997)]. Because all nucleosides are in the standard *anti* conformation (average χ angle 191°), the phenyl C-nucleoside fits seamlessly into the RNA A-duplex. Although the stereoelectronic effects present in the natural pyrimidines and the phenyl ribonucleoside differ significantly, conformational preferences of the latter at the nucleoside level are obviously outweighed by the ribonucleotides bracketing the phenyl residue.

Among helical parameters, significant differences between the native and phenyl-modified RNA duplexes are observed for rise and inclination (Fig. 3A). The average helical rise in the modified duplex is increased by more than 0.5 Å and the inclination is reduced by more than 10°. However, it is unlikely that these changes are a consequence of the phenyl modifications. The earlier finding that the native octamer duplex crystallized in a hexagonal lattice also displayed a rise of around 3.1 Å (Portmann et al., 1995) provides evidence that the RNA duplex itself shows considerable conformational flexibility. The helical parameters depicted in Figure 3A also reveal a slight reduction of the helical rise between the central P-P pair and the flanking C-G pairs. This is accompanied by sharply reduced values for the roll between these base pairs. Other parameters such as slide, displacement, and propeller twist display only minor deviations among the two duplexes.

Consistent with the rather similar overall geometries, the backbone torsion angles in the two duplexes differ only moderately. In the phenyl-modified duplex all nucleotides conform to the standard *sc*⁻, *ap*, *sc*⁺, *sc*⁺, *ap*, *sc*⁻ (α to ζ) genus. Thus, the extended backbone variant adopted by a single nucleotide in the native duplex is not observed in the phenyl-modified one. Taken together, the hydrophobic P-P pair can be accommodated in an RNA duplex without significantly affecting geometry and topology.

Structure and stability

Incorporation of a phenyl residue in place of C4 in the r(CCCCGGGG) octamer leads to loss of Watson-Crick hydrogen bonds and goes along with changes in intra- and interstrand stacking interactions and hydration. A comparison of the thermodynamics of duplex formation for the native RNA and two modified octamers containing a single phenyl at either position 2 or

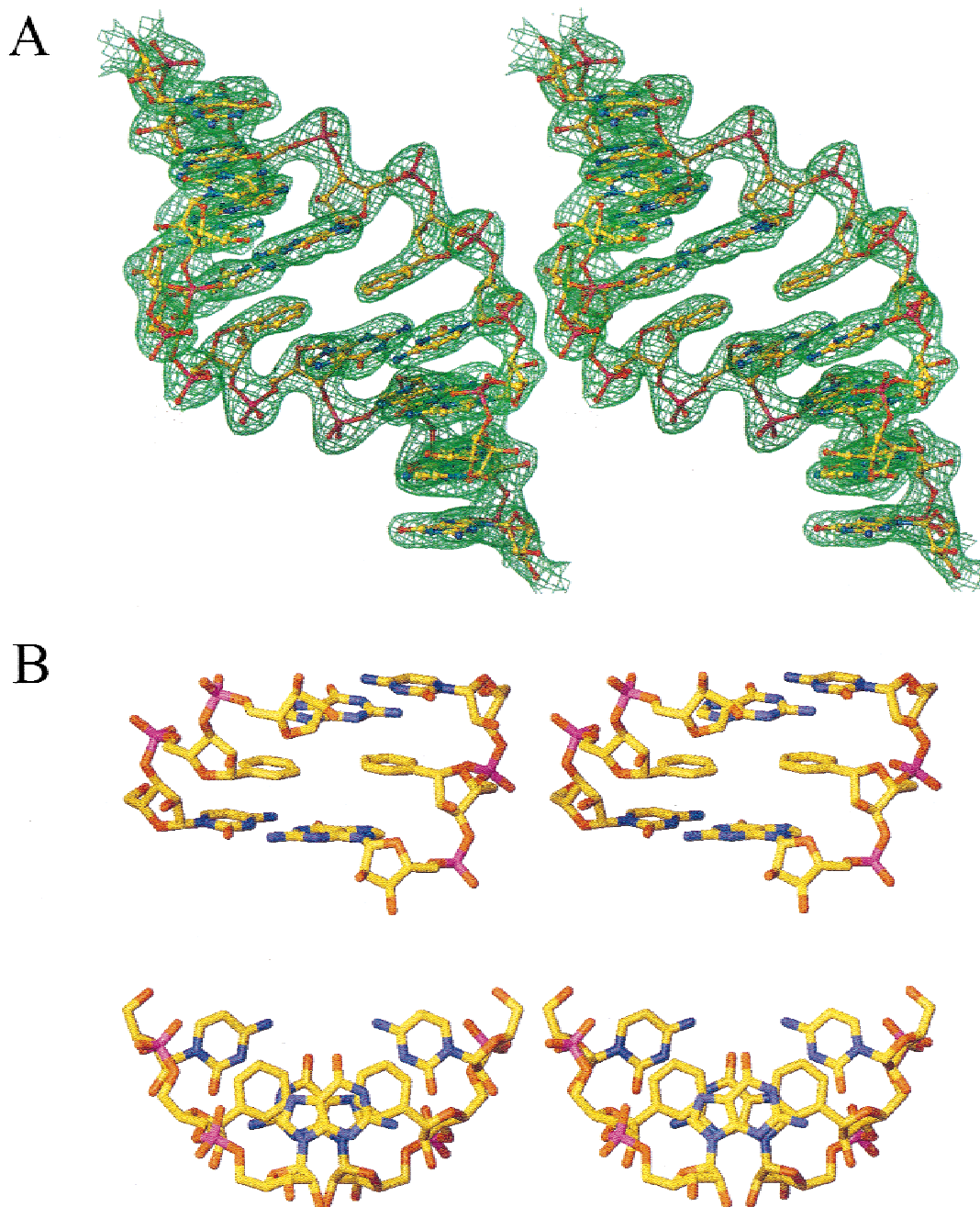


FIGURE 2. A: $(2F_{obs} - F_{calc})$ Fourier sum electron density (green, 1σ -level) drawn around the final model. **B:** Stereo diagrams of the three central base pairs of the $[r(CCCPGGGG)]_2$ duplex, viewed roughly along the crystallographic twofold axis and into the minor groove (top), and along the helical axis (bottom). RNA atoms are colored yellow, red, blue, and magenta for carbon, oxygen, nitrogen, and phosphorus, respectively.

4 is given in Table 1. Accordingly, incorporation of the phenyl moiety leads to a drastic loss in stability in both cases. The changes of around +25 kcal/mol in the enthalpy term for duplex formation are consistent with unfavorable stacking interactions and absence of Watson–Crick hydrogen bonds between phenyls and between phenyl and guanine in the $[r(CCCPGGGG)]_2$ and $[r(CPCCGGGG)]_2$ duplexes, respectively. However, formation of the modified duplexes goes along

with favorable entropic contributions relative to the native RNA octamer.

Inspection of the structure reveals that there is no overlap between phenyls and 5'-cytosines and that the dispersive contributions to stacking between phenyls and 3'-guanines are probably rather limited. As shown in Figures 2B and 3B, the lack of exocyclic functions with phenyl allows only for van der Waals contacts between the C2-C3 and N7-C8 edges of P and G,

TABLE 1. Melting temperatures and thermodynamic data of the octamers.^a

RNA sequence ^b	T_m^c [°C]	$-\Delta H^\circ$ [kcal/mol]	$-\Delta S^\circ$ [cal/mol K]	$-\Delta G_{37}^\circ$ [kcal/mol]
CCCCGGGG	73.3	84.1	220	16.1
CPCCGGGG	37.7	57.8	163	7.3
CCCPGGGG	40.1	60.5	170	7.8

^aError limits for these experiments are $\pm 0.5^\circ\text{C}$ in T_m and $\pm 10\%$ for the thermodynamic values.

^bThe letter P denotes substitution of cytosine with the phenyl moiety.

^cMeasurement conditions were 8 μM total strand concentration, 10 mM sodium phosphate buffer, pH 7, 100 mM total sodium (supplemented as NaCl) and 1 mM EDTA.

respectively. This orientation places the hydrogen of phenyl-C3 above the five-membered ring of guanine (Fig. 3B), likely resulting in a favorable electrostatic contribution to stacking. However, these interactions cannot compensate for the loss of the extensive inter-strand stacking between guanines at the central CpG step in the native duplex (Fig. 3D). The shift between strands avoids positioning of the hydrophobic base analogs opposite guanines. Instead of formation of two P-G pairs, Ps are arranged opposite each other in the center and unpaired guanines stack at both ends of the duplex (Fig. 1B, right). In DNA, hydrophobic base analogs prefer pairing with each other over pairing with natural bases (Schweitzer & Kool, 1995; reviewed in Turner, 1996). Our structure suggests that hydrophobic residues may exhibit a similar selectivity in the case of RNA.

It is likely that the shift between strands that generates the P-P pair is further facilitated by the formation of 3'-terminal unpaired guanines (Figs. 1B, 4A,B). Among the possible dangling-end arrangements involving natural bases, 3'-terminal purines afford the greatest stability, followed by 3'-terminal pyrimidines and 5'-terminal purines (Petersheim & Turner, 1983; Sugimoto et al., 1987). Using hexose-oligonucleotide analogs, Eschenmoser and coworkers demonstrated that the different stabilities provided by 5'- and 3'-overhanging residues are correlated with the degree of inclination between backbone and bases (Micura et al., 1999). Similarly, the base-backbone inclination present in natural RNA duplexes leads to more optimal intra- and interstrand stacking interactions between a 3'-terminal unpaired base and an adjacent base pair (Fig. 1B, right) compared to the corresponding situation for a 5'-overhanging base.

Hydration

The current model of the phenyl-modified RNA duplex comprises 46 water molecules. Most of these are coordinated to Ca^{2+} ions or are part of the first hydration

shell. As expected, the presence of the hydrophobic analogs prevents water molecules from binding near the floors of the major and minor grooves in the central section of the duplex. However, water molecules span the minor groove at its periphery, using the 2'-hydroxyl groups of phenyl nucleosides and 4'-oxygens of 5'-adjacent cytosines as bridge heads (Fig. 4C). This observation provides evidence that the phenyl analog may only distort hydration locally. Although the resolution of the model does not permit visualization of all first-shell water molecules, the water structure around neighboring bases may not be altered significantly as a result of phenyl incorporation and global water networks such as those present in the duplex grooves may not undergo substantial rearrangements either.

Structure and function

A hammerhead ribozyme with a phenyl residue incorporated at position 17, adjacent to the cleavage site, had displayed a surprisingly rapid catalytic rate considering the lack of exocyclic functions with the analog (Baidya et al., 1997; see this reference for a secondary structure schematic of the hammerhead-substrate complex). Replacement of another key residue near the active site, U7, by phenyl even led to a nearly twofold rate enhancement (Burgin et al., 1996). In one of the crystal structures that was determined for hammerhead-substrate complexes, the active site nt 17 and the adjacent nt 1.1 are dC and dG, respectively [the inhibitor strand is composed of 2'-deoxyribonucleotides (Pley et al., 1994)]. Although residue 1.1 was A instead of G and the substrate strand was RNA, the structure of a second hammerhead construct displayed an active-site conformation that was similar to the one in the above ribozyme-inhibitor complex (Scott et al., 1995).

A comparison between the geometries of the CpG steps in the structures of the $[\text{r}(\text{CCCPGGGG})]_2$ duplex and the hammerhead-inhibitor complex is depicted in Figure 3 (panels B and C, respectively). In the ground state, the CpG dimer at the hammerhead active site adopts a nearly canonical A-form helix geometry. As can be seen from the diagrams in Figures 3B and 3C, the geometries of the PpG and dC17pdG1.1 dimers in the two structures are therefore very similar. The hydrogen bond between N4 of C17 and O2 of C3 observed in the crystal structure is disrupted as a result of the C17 \rightarrow P17 mutation. The only other difference may arise from a somewhat reduced overlap between the stacked bases in the case of the PpG step. However, it was shown that C17 modifications do not appear to affect the hammerhead ground-state structures; rather, the exocyclic functions of cytosine are involved in the stabilization of the transition-state structure (Baidya et al., 1997). This is consistent with our observation that the phenyl residue does not cause any significant changes of the helix geometry in a duplex.

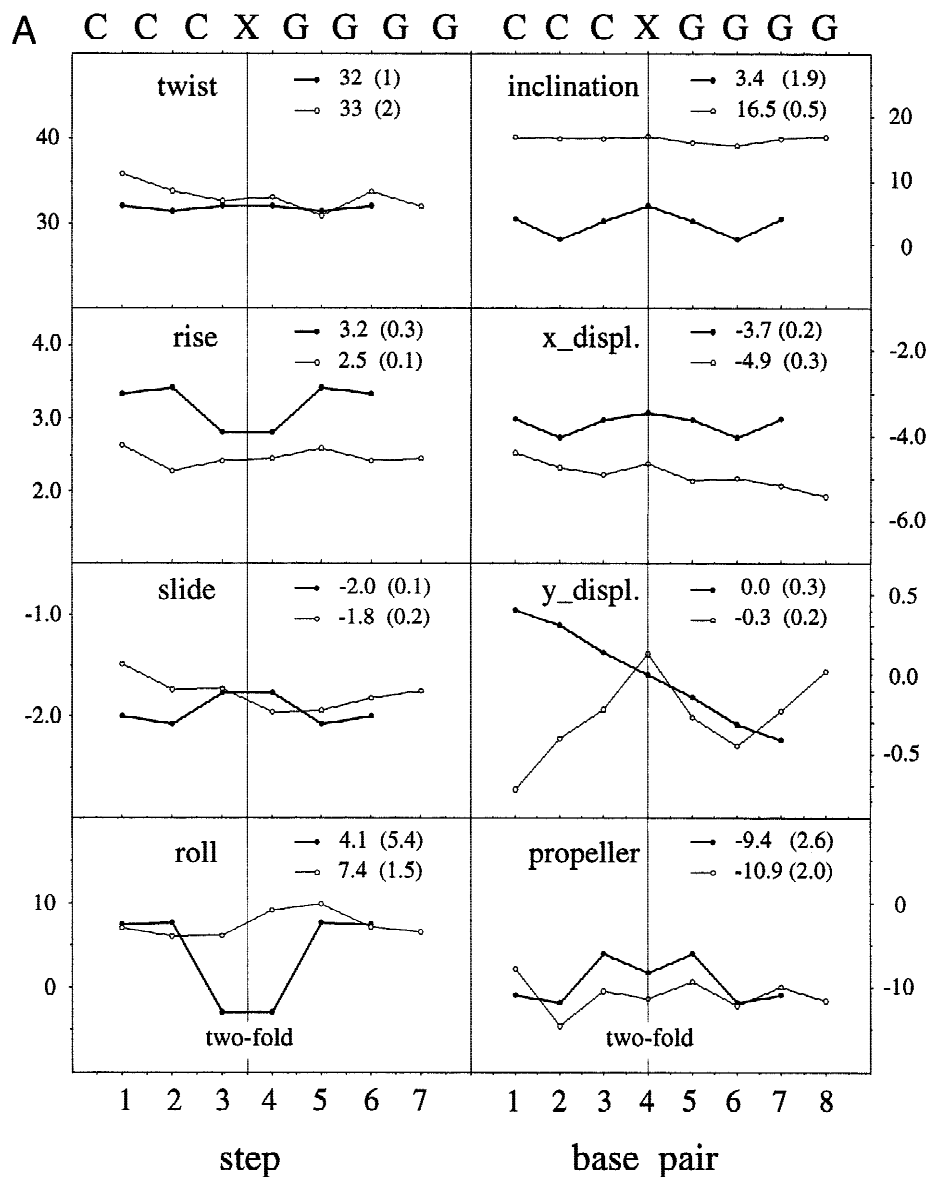
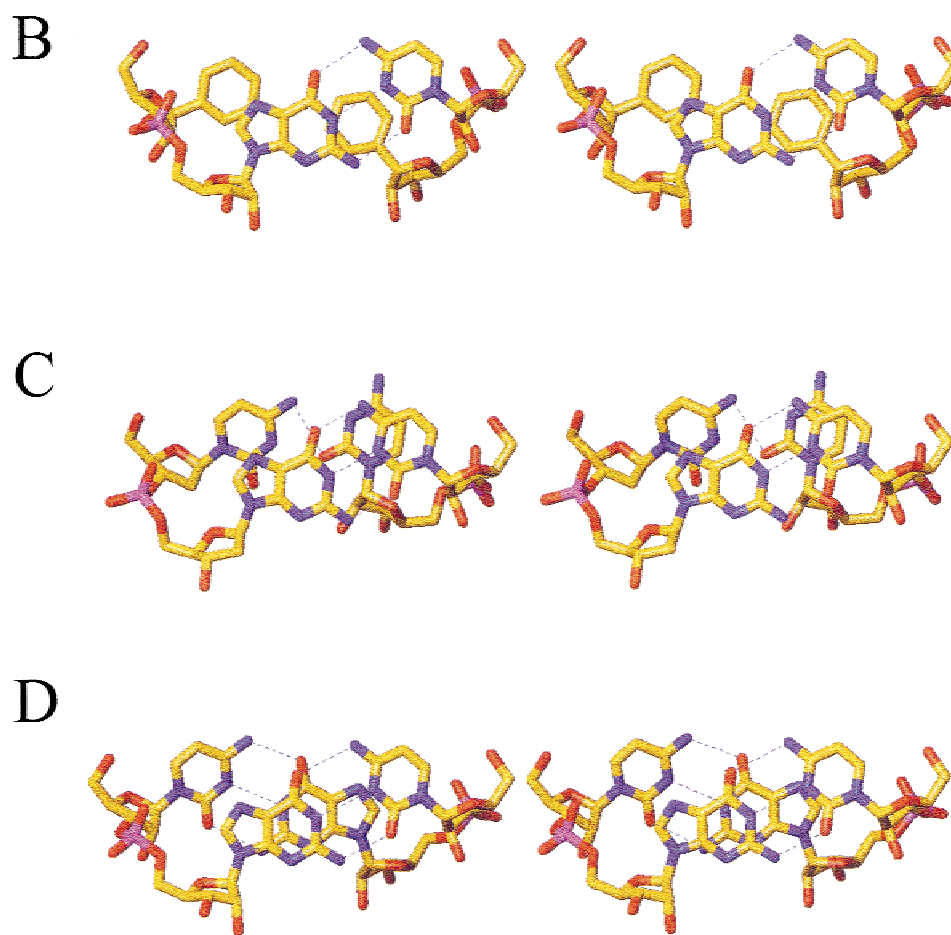


FIGURE 3. A: Geometries of base steps and base pairs in the $[r(\text{CCCCGGGG})_2]$ [$X = C$ (Egli et al., 1996)] and $[r(\text{CCCPGGGG})_2]$ [$X = P$] duplexes (thin and thick lines, respectively). Average values and standard deviations (in parentheses) for individual parameters are listed in the upper right corners, and the thin line marked "two-fold" refers to the location of the crystallographic twofold rotation axis with the $[r(\text{CCCPGGGG})_2]$ duplex. All values were calculated with the program CURVES (Lavery & Sklenar, 1989, 1997). Geometries of the 5'-XpG step in the $[r(\text{CCCPGGGG})_2]$ duplex (**B**) ($X = P$), the hammerhead ribozyme (**C**) [$X = dC$; the cleavage site residues dC17 (opposite C3) and dG1.1 (opposite C2.1); Pley et al., 1994], and the $[r(\text{CCCCGGGG})_2]$ duplex (**D**) ($X = C$; rhombohedral crystal form; Egli et al., 1996). RNA atoms are colored yellow, red, blue, and magenta for carbon, oxygen, nitrogen, and phosphorus, respectively, and hydrogen bonds are drawn as thin dashed lines. (Figure continues on facing page.)

Shape and stacking features of the base at position 17 appear to be more important than whether or not it can engage in hydrogen-bonding interactions.

The conformational changes required to bring about the in-line orientation of the 2'-oxygen of C17 and the scissile bond in the substrate strand are accompanied by unstacking of the cytosine base and the adjacent adenine 1.1 [sequence refers to the above RNA-substrate complex (Scott et al., 1995)] (Scott et al., 1996; Murray et al., 1998). Because the overlaps between bases at the PpG and CpG steps in the phenyl-

modified duplex and at the hammerhead active site, respectively, indicate a somewhat less optimal interaction with phenyl, the C17P mutation may actually facilitate the unstacking of bases that precedes the cleavage step. Although the lack of exocyclic functions proves to be a disadvantage for the phenyl residue in the stabilization of the transition state, its enhanced flexibility compared with a slightly more bulky and hydrogen-bonded cytosine may contribute to the relatively high catalytic rate of the phenyl-modified hammerhead. Other changes with phenyl compared to

FIGURE 3. *Continued.*

cytosine that may affect the role of the former in the pathway from the ground state to a catalytically competent conformation concern hydration and the creation of a potentially lower dielectric environment (Baidya et al., 1997, and cited references). Based on the water structure observed around the P-P pair in the minor groove of the modified RNA duplex, water molecules may be expelled from regions in the immediate vicinity of the phenyl moiety. However, the sugar of the phenyl residue can still participate in hydrogen-bonding networks that involve water molecules via its 4'-oxygen and the 2'-hydroxyl group. Alternatively, it is possible that water is not an important player in the conformational changes of residue 17 that occur during line-up of 2'-OH and scissile bond. Another stabilizing interaction mediated by phenyl that could compensate for the loss of hydrogen-bonding interactions is quadrupolar effects resulting from an edge-to-face orientation between aromatic species (Burley & Petsko, 1985).

Lattice interactions and Ca^{2+} coordination

The two Ca^{2+} ions per crystallographic asymmetric unit stabilize stacking interactions between duplexes

as well as lateral contacts between duplexes from neighboring stacks (Fig. 4A,B). Each duplex exhibits direct or water-mediated contacts to eight Ca^{2+} ions. Ca1 displays a pentagonal bipyramidal coordination geometry and mediates contacts between three strands from three different duplexes. Ca2 sits on a crystallographic twofold rotation axis and displays regular octahedral coordination geometry. It bridges phosphate groups of 3'-terminal stacked guanines from adjacent duplexes. A summary of the calcium-oxygen distances is listed in Table 2.

Ca1 is involved in three inner-sphere contacts to RNA atoms, the first two to the O2' and O3' atoms of the 3'-terminal guanosine and a third to the O1P atom of residue P4 from a second duplex (Fig. 4A). The remaining four ligands are water molecules that in turn are hydrogen bonded to RNA atoms with the exception of W11. W13 bridges O2P atoms of residues G7 and G8 from a third duplex, W10 is hydrogen bonded to N7 of G8 from the same strand and W12 is hydrogen bonded to O1P of C3 from duplex 2. Thus, O2'(G8), O3'(G8), W11, W12, and W13 form the equatorial pentagon of the Ca1 coordination sphere and O1P(P4a) and W10 are the apical ligands (lower case letters in

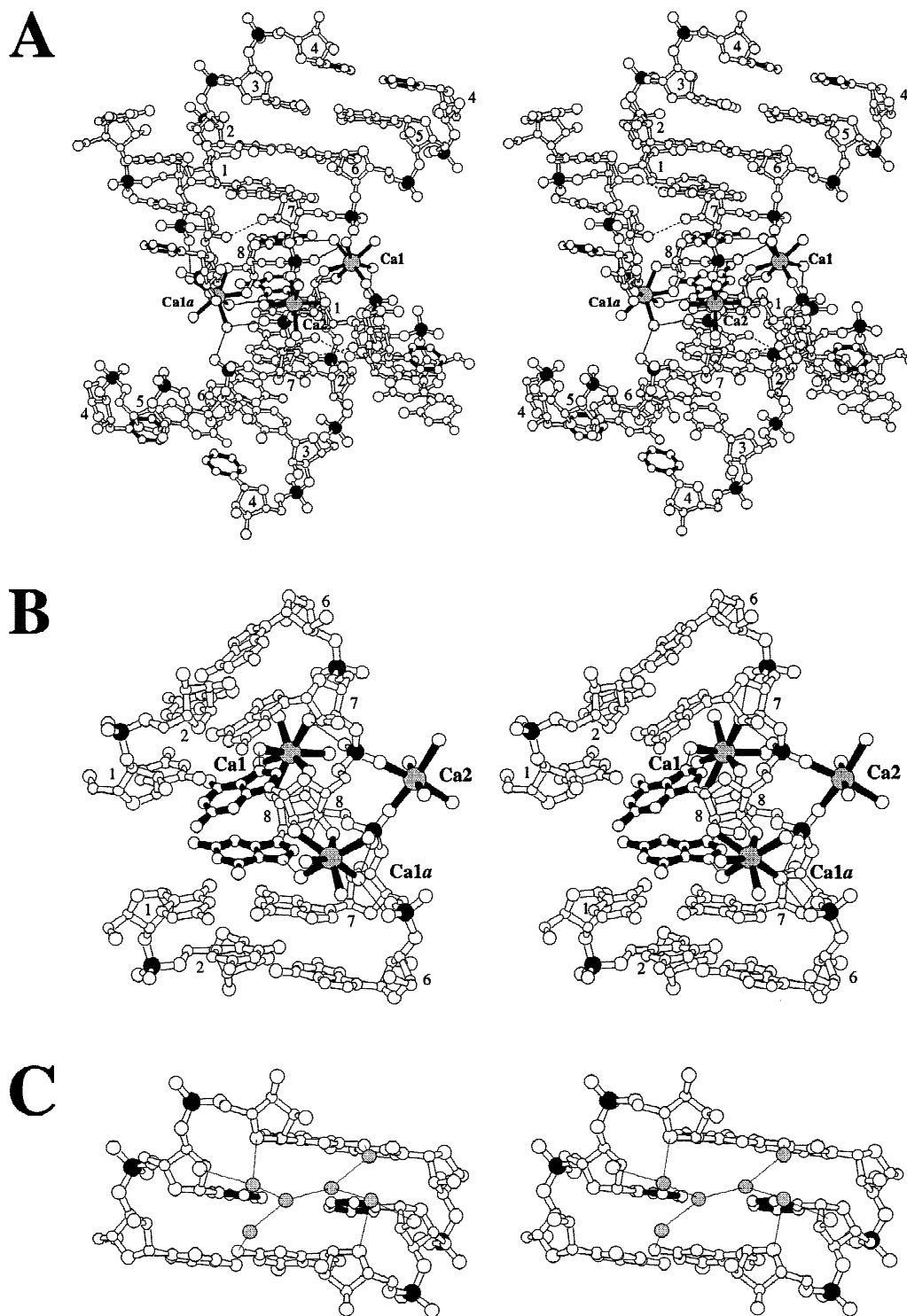


FIGURE 4. **A:** Stereo diagram of Ca^{2+} ions stabilizing stacked terminal guanines (Ca1 and Ca2) and mediating lateral contacts between duplexes (Ca1). Ca1 and Ca1a are symmetry related and Ca2 is located on a crystallographic twofold rotation axis. **B:** Close-up view of the coordination modes of the three Ca^{2+} ions at the interface between stacked duplexes. RNA strands are drawn with open bonds and phosphorus atoms are drawn as filled circles. Phenyls and stacked guanines are highlighted with solid bonds, Ca^{2+} ions are stippled in gray, calcium-oxygen bonds are filled and selected residues are numbered. **C:** Stereo diagram of the water structure in the central portion of the RNA minor groove. Water molecules bridge 2'-hydroxyl groups and 4'-oxygens from opposite strands across the groove. Waters are drawn as gray spheres, phenyls are highlighted with solid bonds, and hydrogen bonds are thin solid lines. The temperature factors of many water molecules indicate that their sites are only partially occupied.

TABLE 2. Geometry of Ca²⁺ coordination.

Ion	Distance [Å]	Ligand DNA/water
Ca1	2.5	O2' G8
	2.3	O3' G8
	2.6	O1P P4(a) ^a
	2.4	W10
	2.3	W11
	2.6	W12
	2.6	W13
	Ca2 ^b	2.4
2.6		W15
2.3		W16

^aSymmetry-related strand.^bCa2 is located on a twofold axis.

italics designate atoms from symmetry related strands). Ca2 is coordinated to four water molecules and in addition forms two inner-sphere contacts by clamping onto symmetry-related phosphates from unpaired 3'-terminal guanosines. The bases of the two latter residues exhibit a strong tilt (Fig. 4B), possibly a consequence of the particular coordination modes of the three Ca²⁺ ions at the interface between stacked duplexes. In addition to being stabilized by Ca2, lateral contacts between duplexes in the minor grooves are also mediated by a hydrogen bond between 2'-hydroxyl groups (residues C3a and G7; dashed line, Fig. 4A) and a further hydrogen bond between the 2'-OH of residue C2a and N2 of the above guanine.

CONCLUSIONS

The crystal structure of an RNA duplex with incorporated phenyl ribonucleotides determined at a resolution of 1.97 Å reveals that the phenyl analog can stack between bases, resulting only in minor deviations from a standard A-form geometry of the duplex. In the crystallized sequence, phenyls are arranged opposite each other forming a pseudo-base pair with van der Waals contacts between phenyl rings across strands. The preferred pairing between hydrophobic base analogs observed here is consistent with earlier results in DNA that demonstrated self-pairing between hydrophobic isosteres in DNA duplexes (Schweitzer & Kool, 1995). The structural results suggest that phenyl may be a better mimetic of the natural pyrimidines than one might have expected for a base analog lacking any hydrogen bond donors or acceptors. This is in line with the wild-type activities of hammerhead ribozymes bearing phenyl residues at key sites and the observation that a pre-mRNA substrate with a phenyl instead of A at the 3' splice site is a better substrate than those carrying a G, C, or U substitution (Gaur et al., 2000). Matching shape, enhanced conformational flexibility, and alternative

stacking interactions, involving dipolar and quadrupolar effects, may allow the phenyl analog to overcome the absence of hydrogen-bonding functions and to mimic the interactions of wild-type bases at the active site of ribozymes and spliceosomes.

MATERIALS AND METHODS

Materials

Synthesis of monomer building blocks

NMR spectra were recorded on a Varian Gemini 400 spectrometer operating at 400.075 MHz for proton and 161.947 MHz for phosphorus. Chemical shifts in parts per million refer to TMS and H₃PO₄, respectively. Analytical TLC was performed with Whatman MK6F silica gel 60 Å F₂₅₄ plates and column chromatography using Merck 0.040–0.063 mm Silica gel 60.

2,3,5-tri-O-benzyl-D-ribo-1,4-lactone (2) (Fig. 1A). To a solution of (1) (5.0 g, 33.8 mmol) stirring at 0°C under argon in anhydrous dioxane was added benzyl-2,2,2-trichloroacetimidate (37.0 mL, 253.2 mmol) via syringe. After 10 min, triflic acid (0.25 mL, 5.7 mmol) was added via syringe and the reaction maintained at 0°C for 1 h, then 16 h at room temperature (rt). TLC (25% EtOAc/hexane) indicated complete consumption of (1) $R_f = 0$ and formation of (2) $R_f = 0.5$. Dioxane was removed *in vacuo* and the resulting residue suspended in dichloromethane and filtered to remove excess trichloroacetimide. The filtrate was washed with saturated aqueous (sat. aq.) sodium bicarbonate and the organic layer dried over sodium sulfate, filtered to remove salts, and then evaporated *in vacuo*. Additional trichloroacetimide was removed by filtration from 1:1 dichloromethane/hexane. The filtrate was flash chromatographed using a gradient of 10 to 25% ethyl acetate/hexanes to give (2) with trichloroacetimide contamination. The remaining trichloroacetimide was removed by crystallization at –15°C in dichloromethane followed by filtration. Evaporation of the filtrate *in vacuo* provided pure (2), (12.38 g, 90.8%).

¹H NMR (CDCl₃) δ: 7.47–7.25 (m, 15H, Ph), 4.67 (dd, $J = 11.8, 2\text{H}, \text{CH}_2\text{Ph}$), 4.71 (dd, $J = 12.2, 2\text{H}, \text{CH}_2\text{Ph}$), 4.63 (dd, $J_{4,5} = 2.4, J_{4,3} = 4.0, 1\text{H}, \text{H-4}$), 4.54 (dd, $J = 11.4, 2\text{H}, \text{CH}_2\text{Ph}$), 4.50 (br s, 1H, H-2), 4.19 (dd, $J_{3,2} = 2.0, J_{3,4} = 4.0, 1\text{H}, \text{H-3}$), 3.75 (dd, $J_{5,4} = 2.4, J_{5,5'} = 10.8, 1\text{H}, \text{H-5}$), 3.64 (dd, $J_{5',4} = 2.4, J_{5',5} = 10.8, 1\text{H}, \text{H-5'}$).

1'-deoxy-1'-phenyl-β-D-ribofuranose (5). To a solution of (2) (18.43 g, 44.0 mmol) stirring at –78°C in anhydrous THF (200 mL) under argon was added phenyllithium (27 mL, 48.44 mmol) dropwise via syringe. The reaction mixture was stirred at –78°C for 2 h followed by 4 h at rt before being cooled to 0°C and quenched with ice water. TLC (25% EtOAc/hexane) indicated the formation of a new product $R_f = 0.52$, which charred differently than (2) $R_f = 0.50$. Extraction with diethyl ether (2×) followed by drying over sodium sulfate and evaporation *in vacuo* provided crude hemiacetal (3). This material was dissolved in anhydrous acetonitrile and cooled to –40°C while stirring under argon. Triethylsilane (14.1 mL,

88 mmol) was added followed by dropwise addition of boron trifluoride etherate (6.14 mL, 48.44 mmol) over 30 min. After stirring at -40°C for 1 h, the reaction mixture was allowed to warm to 0°C , at which time sat. aq. potassium carbonate solution (85 mL) was added to quench the reaction. TLC (10% EtOAc/hexane) indicated the disappearance of (3) $R_f = 0.22$ and formation of intermediate (4) $R_f = 0.50$. Extraction with diethyl ether ($2\times$) and drying over sodium sulfate followed by filtration and drying *in vacuo* provided intermediate (4) (9.75 g, 20.3 mmol, 46% over two steps). To a solution of (4) stirring at -78°C under argon in anhydrous dichloromethane was added boron tribromide (1 M in DCM) (51.0 mL, 50.75 mmol) dropwise via syringe. The reaction was stirred for 2.5 h at -78°C and was then quenched with a 1:1 solution of methanol/dichloromethane. TLC (10% EtOH/ CH_2Cl_2) indicated the disappearance of (4) $R_f = 0.22$ and formation of product (5) $R_f = 0.49$. Treatment with pyridine (50 mL) followed by evaporation *in vacuo* and flash chromatography (5–15% EtOH/DCM) provided (5), (2.91 g, 68%).

Melting point: $120\text{--}121^{\circ}\text{C}$ (literature mp $120\text{--}121^{\circ}\text{C}$). ^1H NMR ($\text{DMSO-}d_6 + \text{D}_2\text{O}$) δ : 7.47–7.31 (m, 5H, Ph), 4.63 (d, $J_{1,2'} = 7.0$, 1H, H-1'), 3.95 (dd, $J_{3,2'} = 5.4$, $J_{3,4'} = 3.7$, 1H, H-3'), 3.89 (dd, $J_{4,5'} = 4.4$, 1H, H-4'), 3.76 (dd, $J_{2,1'} = 7.0$, $J_{2,3'} = 5.4$, 1H, H-2'), 3.61 (m, 2H, H-5', H-5'').

3'-O-t-Butyldimethylsilyl-5'-O-dimethoxytrityl-1'-deoxy-1'-phenyl- β -D-ribofuranose (6b) and 2'-O-t-butyl-dimethylsilyl-5'-O-dimethoxytrityl-1'-deoxy-1'-phenyl- β -D-ribofuranose (6a). Compound 5 (770 mg, 3.7 mmol) was 5'-O-dimethoxytritylated according to standard procedures (Matulic-Adamic et al., 1996) to yield, after silica gel column chromatography (0.5–2% gradient of ethyl acetate in hexane), 1.4 g (75% yield) of 5'-O-dimethoxytrityl derivative as a yellowish foam. The above material (1.4 g, 2.73 mmol) was treated with *t*-butyldimethylsilyl chloride using standard procedures (Matulic-Adamic et al., 1996) and products were purified by silica gel column chromatography (1–2% gradient of ethyl acetate in hexane) to afford the faster moving 3'-O-TBDMSi isomer 6b as a foam (0.55 g, 32%).

The slower migrating 2'-O-TBDMSi isomer 6a was then eluted to give, upon evaporation, a white foam (0.60 g, 35%). The 3'-O-TBDMSi isomer 6b was isomerized in a solution of 5% Et_3N in methanol (50 mL) for 1 h at rt, providing a 1:1 mixture of the 2'- and 3'-isomers 6a and 6b. Column chromatography of this mixture under conditions described above allows for isolation of an additional 0.25 g of 6a.

RNA synthesis and purification

Oligonucleotide syntheses were carried out on a 2.5 μmol scale (Pharmacia Expedite), using standard 2'-O-(*t*-butyldimethyl)-silyl- (TBDMS-) modified phosphoramidite building blocks (Wincott et al., 1995). Two modified oligoribonucleotides were produced: r(CPCCGGGG) and r(CCCPGGGG). The CPG-bound octamers were deprotected in ethanolic ammonia at 55°C overnight. The TBDMS groups were removed at rt in a 1 M solution of tetra-*n*-butylammonium fluoride in tetrahydrofuran. Both deprotected strands were purified by high performance liquid chromatography (HPLC, reverse phase C-18 column, 50 mM triethylammonium buffer, pH 7, acetonitrile eluent). After lyophilization the stock concentrations for both were adjusted to 10 mM in water (single strand).

Methods

Crystallization

Crystallization conditions were screened with sparse matrix kits (Jancarik & Kim, 1991) both at rt and 4°C , using the hanging drop vapor diffusion technique. Although no crystals were obtained with the CPCCGGGG oligonucleotide, diffraction-quality crystals could be grown for r(CCCPGGGG) with buffer No. 46 (Crystal Screen I, Hampton Research, Laguna Niguel, California) in the cold room. A 10- μL droplet containing 1.5 mM RNA, 50 mM calcium acetate, 25 mM sodium cacodylate, pH 6.5, and 4.5% (v/v) PEG 8000 was equilibrated against a 0.5 mL reservoir solution (0.2 M calcium acetate, 0.1 M sodium cacodylate, pH 6.5, and 18% PEG 8000) and crystals appeared within two weeks.

Data collection and processing

Crystals were stabilized in reservoir buffer supplemented by 25% glycerol, mounted in nylon loops and frozen and stored in liquid nitrogen. Data were collected on the insertion device (ID) beamline of the DuPont-Northwestern-Dow Collaborative Access Team (DND-CAT) at sector 5 of the Advanced Photon Source (Argonne, Illinois). A crystal was transferred into the nitrogen stream and separate high-resolution (200 frames, oscillation angle 0.5°) and low-resolution (60 frames, oscillation angle 1.5°) data sets were collected at a wavelength of 1.0004 \AA , using a MARCCD detector. The high-resolution images revealed strong anisotropy of the diffraction pattern, with reflections of up to 1.6 \AA resolution along the stacking direction of duplexes (long cell dimension in the *z*-direction, Table 3). Data were integrated and scaled in the DENZO/SCALEPACK suite (Otwinowski & Minor, 1997)

TABLE 3. Crystal data and selected data collection and refinement parameters.

Space group	$P6_122$
$a = b$ [\AA]	24.31
c [\AA]	123.79
Data collection	
X-ray source	ID-5, APS
Temperature [K]	100
Total no. of reflections	25,862
No. of unique reflections	1,904
Resolution [\AA]	1.97
Mean $I/\sigma(I)$	20.5
Completeness (2.0–1.97 \AA shell) [%]	99.1 (99.5)
R_{merge} (2.0–1.97 \AA shell) [%]	4.6 (24.3)
Refinement	
No. of reflections ($I > 0$)	1,736
Working set	1,551
Test set	185
No. of RNA atoms	167
No. of Ca^{2+} ions	2
No. of water molecules	46
R -factor working set [%]	21.7
R -factor test set [%]	26.9
Rms bond lengths [\AA]	0.009
Rms bond angles [deg]	1.40

with a cut-off limit at 1.97 Å. Crystal data and selected data collection statistics are summarized in Table 3.

Structure determination and refinement

The structure was determined by the Molecular Replacement technique [program AMoRe (Navaza, 1994)], using models with a variety of secondary structures (Fig. 1B) and varying the helical rise of the duplex portions. Crystallographic refinement was conducted with the program CNS (Brünger, 1998), setting aside 10% of the reflections to calculate the R_{free} (Brünger, 1992). Updated dictionaries for bond lengths and angles were used (Parkinson et al., 1996) and the geometric parameters for the P residue were taken from the crystal structure of the phenyl nucleoside (Matulic-Adamic et al., 1996). Following initial cartesian and B-factor refinement cycles, the model was improved by simulated annealing. At this stage, Fourier electron density maps displayed on a Silicon Graphics computer with the program TURBO-FRODO (Cambillau & Roussel, 1997) revealed two hydrated Ca^{2+} ions. The ions were placed in the maps along with 46 water molecules and the model was further refined. After the refinement converged, reflections in the 1.97–1.60 Å resolution range ($F \geq 0$, completeness 50%) were included in the refinement. However, this did not result in a notable improvement of the model or the determination of further water molecules bound to RNA and, therefore, the data cut-off limit was kept at 1.97 Å. Final refinement parameters and root mean square (rms) deviations from standard bond lengths and angles are listed in Table 3 and a stereo diagram of the $(2F_{obs} - F_{calc})$ sum electron density surrounding the final model is depicted in Figure 2A.

UV-melting experiments

Melting temperatures were measured on a Beckman DU-7500 UV spectrophotometer, equipped with a Peltier thermal control unit. Equilibrium melting curves of native and chemically modified RNA octamers in buffered solutions with concentrations between 4 and 24 μ M were recorded. The buffer consisted of 10 mM sodium phosphate, pH 7.0, with the total Na^+ concentration being 100 mM (supplemented as NaCl), and 1 mM EDTA. The lower temperature limit was 15 °C, the upper temperature limit was 95 °C, and the temperature increment was 0.5 °C, with an equilibration time of 30 s. Thermodynamic parameters were extracted from $1/T_m$ versus $\ln[c]$ plots assuming a two-state model (Marky & Breslauer, 1987). All plots were analyzed by linear regression.

Coordinates

Structure factor data and coordinates for the final model have been deposited in the Protein Data Bank (PDB ID code 1G2J).

ACKNOWLEDGMENTS

We would like to thank Dr. Stefan Portmann for help with RNA purification and crystallization and Dr. Valentina Tereshko for helpful discussions. This work was supported by National Institutes of Health Grant GM55237 (M.E.) and fi-

ancial support in the form of a Natural Sciences and Engineering Research Council of Canada fellowship to C.J.W. is gratefully acknowledged. The DuPont-Northwestern-Dow Collaborative Access Team Synchrotron Research Center at the Advanced Photon Source, Argonne, Illinois, is supported by E.I. DuPont de Nemours & Co., The Dow Chemical Company, the National Science Foundation and the State of Illinois.

Received June 14, 2000; returned for revision July 10, 2000; revised manuscript received July 26, 2000

REFERENCES

- Baidya N, Ammons GE, Matulic-Adamic J, Karpeisky AM, Beigelman L, Uhlenbeck OC. 1997. Functional groups on the cleavage site pyrimidine nucleotide are required for stabilization of the hammerhead transition state. *RNA* 3:1135–1142.
- Bennett CF, Cowser LM. 1999. Antisense oligonucleotides as a tool for gene functionalization and target validation. *Biochim Biophys Acta* 1489:19–30.
- Blättler MO, Wenz C, Pingoud A, Benner SA. 1998. Distorting duplex DNA by dimethylsulfone substitution: A new class of "transition state analog" inhibitors for restriction enzymes. *J Am Chem Soc* 120:2674–2675.
- Brünger AT. 1992. Free R value: A novel statistical quantity for assessing the accuracy of crystal structures. *Nature* 355:472–475.
- Brünger AT. 1998. Crystallography & NMR System (CNS), Version 0.4, Yale University, New Haven, CT.
- Burgin AB Jr, Gonzalez C, Matulic-Adamic J, Karpeisky AM, Usman N, McSwiggen JA, Beigelman L. 1996. Chemically modified hammerhead ribozymes with improved catalytic rates. *Biochemistry* 35:14090–14097.
- Burley SK, Petsko GA. 1985. Aromatic-aromatic interaction—A mechanism of protein-structure stabilization. *Science* 229:23–28.
- Cambillau C, Roussel A. 1997. Turbo Frodo, Version OpenGL.1, Université Aix-Marseille II, Marseille, France.
- Cate JH, Gooding AR, Podell E, Zhou K, Golden BL, Kundrot CE, Cech TR, Doudna JA. 1996. Crystal structure of a group I ribozyme domain: Principles of RNA packing. *Science* 273:1678–1685.
- Crooke ST, ed. 1998. *Handbook of experimental pharmacology, Vol. 131, Antisense research and applications*. Berlin and Heidelberg: Springer Verlag.
- Czernecki S, Ville G. 1989. C-glycosides. 7. Stereospecific C-glycosylation of aromatic and heterocyclic rings. *J Org Chem* 54:610–612.
- Deng L, Schäfer OD, Verdine GL. 1997. Unusually strong binding of a designed transition-state analog to a base-excision DNA repair protein. *J Am Chem Soc* 119:7865–7866.
- Egli M, Portmann S, Usman N. 1996. RNA hydration: A detailed look. *Biochemistry* 35:8489–8494.
- Elghanian R, Storhoff JJ, Mucic RC, Letsinger RL, Mirkin CA. 1997. Selective colorimetric detection of polynucleotides based on the distance-dependent optical properties of gold nanoparticles. *Science* 277:1078–1081.
- Eschenmoser A. 1999. Chemical etiology of nucleic acid structure. *Science* 284:2118–2124.
- Gaur RK, Beigelman L, Haeberli P, Maniatis T. 2000. Role of adenine functional groups in the recognition of the 3'-splice-site AG during the second step of pre-mRNA splicing. *Proc Natl Acad Sci USA* 97:115–120.
- Guckian KM, Krugh TR, Kool ET. 1998. Solution structure of a DNA duplex containing a replicable difluorotoluene-adenine pair. *Nature Struct Biol* 5:954–959.
- Guckian KM, Schweitzer BA, Ren RX-F, Sheils CJ, Tahmassebi DC, Kool ET. 2000. Factors contributing to aromatic stacking in water: Evaluation in the context of DNA. *J Am Chem Soc* 122:2213–2222.
- Hall J, Hüsken D, Häner R. 1996. Towards artificial ribonucleases: The sequence-specific cleavage of RNA in a duplex. *Nucleic Acids Res* 24:3522–3526.
- Jancarik J, Kim S-H. (1991). Sparse matrix sampling: A screening

- method for crystallization of proteins. *J Appl Crystallogr* 24:409–411.
- Jensen HS, Limberg G, Pedersen C. 1997. Benzoylation of aldono-lactones with benzyl trichloroacetimidate. *Carbohydr Res* 302:109–112.
- Lavery R, Sklenar H. 1989. Defining the structure of irregular nucleic acids—conventions and principles. *J Biomol Struct Dyn* 6:655–667.
- Lavery R, Sklenar H. 1997. CURVES 5.2: Helical analysis of irregular nucleic acids. Paris, France: Laboratoire de Biochimie Theoretique, CNRS URA 77, Institut de Biologie Physico-Chimique.
- Marky LA, Breslauer KJ. 1987. Calculating thermodynamic data for transitions of any molecularity from equilibrium melting curves. *Biopolymers* 26:1601–1620.
- Marquez VE, Ezzitouni A, Russ P, Siddiqui MA, Ford H Jr, Feldman RJ, Mitsuya H, George C, Barchi JJ Jr. 1998. HIV-1 reverse transcriptase can discriminate between two conformationally locked carbocyclic AZT triphosphate analogues. *J Am Chem Soc* 120:2780–2789.
- Matray TJ, Kool ET. 1998. Selective and stable DNA base pairing without hydrogen bonds. *J Am Chem Soc* 120:6191–6192.
- Matray TJ, Kool ET. 1999. A specific partner for abasic damage in DNA. *Nature* 399:704–708.
- Matulic-Adamic J, Beigelman L, Portmann S, Egli M, Usman N. 1996. Synthesis and structure of 1-deoxy-1-phenyl- β -D-ribofuranose and its incorporation into oligonucleotides. *J Org Chem* 61:3909–3911.
- Micura R, Kudick R, Pitsch S, Eschenmoser A. 1999. Chemistry of Pyranosyl-RNA, part 8. Chemistry of alpha-aminonitriles, part 24. Opposite orientation of backbone inclination in pyranosyl-RNA and homo-DNA correlates with opposite directionality of duplex properties. *Angew Chem Intn Ed Engl* 38:680–683.
- Morales JC, Kool ET. 1998. Efficient replication between non-hydrogen-bonded nucleoside shape analogs. *Nature Struct Biol* 5:950–954.
- Moran S, Ren RX-F, Rumney IV S, Kool ET. 1997. Difluorotoluene, a nonpolar isostere for thymine, codes specifically and efficiently for adenine in DNA replication. *J Am Chem Soc* 119:2056–2057.
- Murray JB, Terwey DP, Maloney L, Karpeisky A, Usman N, Beigelman L, Scott WG. 1998. The structural basis of hammerhead ribozyme self-cleavage. *Cell* 92:665–673.
- Myers KJ, Dean NM. 2000. Sensible use of antisense: How to use oligonucleotides as research tools. *Trends Pharmac Sci* 21:19–23.
- Navaza J. 1994. AMoRe: An automated package for molecular replacement. *Acta Cryst A* 50:157–163.
- Nielsen PE, ed. 1999. Gene structure and expression. *Biochim Biophys Acta* 1489:1–206.
- Ogawa AK, Wu Y, McMinn DI, Liu J, Schultz PG, Romesberg FE. 2000. Efforts toward the expansion of the genetic alphabet: Information storage and replication with unnatural hydrophobic base pairs. *J Am Chem Soc* 120:11586–11587.
- Ogilvie KK. 1983. The alkylsilyl protecting groups: In particular, the tert-butylidimethylsilyl group in nucleoside and nucleotide chemistry. In: Rideout JL, Henry DW, Beacham LM III, eds. *Nucleosides and nucleotides and their biological applications*. New York: Academic Press. pp 209–256.
- Otwinowski Z, Minor W. 1997. Processing of X-ray diffraction data collected in oscillation mode. *Methods Enzymol* 276:307–326.
- Parkinson G, Vojtechovsky J, Clowney L, Brünger AT, Berman HM. 1996. New parameters for the refinement of nucleic acid containing structures. *Acta Cryst D* 52:57–64.
- Peracchi A, Matulic-Adamic J, Wang S, Beigelman L, Herschlag D. 1998. Structure–function relationships in the hammerhead ribozyme probed by base rescue. *RNA* 4:1332–1346.
- Petersheim M, Turner DH. 1983. Base-stacking and base-pairing contributions to helix stability: Thermodynamics of double-helix formation with CCGG, CCGGp, ACCGGp, ACCGGUp, and ACCGGUp. *Biochemistry* 22:256–263.
- Pley HW, Flaherty KM, McKay DB. 1994. Three-dimensional structure of a hammerhead ribozyme. *Nature* 372:68–74.
- Portmann S, Usman N, Egli M. 1995. The crystal structure of r(CCCCGGGG) in two distinct lattices. *Biochemistry* 34:7569–7575.
- Schweitzer BA, Kool ET. 1995. Hydrophobic, non-hydrogen-bonding bases and base pairs in DNA. *J Am Chem Soc* 117:1863–1872.
- Scott WG, Finch JT, Klug A. 1995. The crystal structure of an all-RNA hammerhead ribozyme: A proposed mechanism for RNA catalytic cleavage. *Cell* 81:991–1002.
- Scott WG, Murray JB, Arnold JRP, Stoddard BL, Klug A. 1996. Capturing the structure of a catalytic RNA intermediate: The hammerhead ribozyme. *Science* 274:2065–2069.
- Strauss JK, Prakash TP, Roberts C, Switzer C, Maher LJ III. 1996. DNA bending by a phantom protein. *Chem Biol* 3:671–678.
- Sugimoto N, Kierzek R, Turner DH. 1987. Sequence dependence for the energetics of dangling ends and terminal base pairs in ribonucleic acid. *Biochemistry* 26:4554–4558.
- Taylor MF, Widerholt K, Sverdrup F. 1999. Antisense oligonucleotides: A systematic high-throughput approach to target validation and gene function determination. *Drug Disc Today* 4:562–567.
- Turner DH. 1996. Thermodynamics of base pairing. *Curr Opin Struct Biol* 6:299–304.
- Wincott FE, DiRenzo A, Shaffer C, Grimm S, Tracz D, Workman C, Sweedler D, Gonzalez C, Scaringe S, Usman N. 1995. Synthesis, deprotection, analysis and purification of RNA and ribozymes. *Nucleic Acids Res* 23:2677–2684.